

## Supporting Information

Huilin Xie,<sup>‡a</sup> Jingtian Zhang,<sup>‡c</sup> Chao Chen,<sup>ac</sup> Feiyi Sun,<sup>a</sup> Haixiang Liu,<sup>b</sup> Xinyuan He,<sup>a</sup> Kristy W. K. Lam,<sup>a</sup> Zhao Li,<sup>a</sup> Jacky W. Y. Lam,<sup>ab</sup> Guo-Qiang Zhang,<sup>\*c</sup> Dan Ding,<sup>c</sup> Ryan T. K. Kwok<sup>\*ab</sup> and Ben Zhong Tang<sup>\*abde</sup>

*<sup>a</sup>Department of Chemistry, Hong Kong Branch of Chinese National Engineering Research Center for Tissue Restoration and Reconstruction, Institute for Advanced Study, The Hong Kong University of Science and Technology (HKUST), Clear Water Bay, Kowloon, Hong Kong, China.*

*<sup>b</sup>HKUST Shenzhen Research Institute, No. 9 Yuexing 1 st RD, South Area Hi-tech Park, Nanshan, Shenzhen 518057, China.*

*<sup>c</sup>Key Laboratory of Bioactive Materials, State Key Laboratory of Medicinal Chemical Biology, Key Laboratory of Functional Polymer Ministry of Education, and College of Life Sciences, Nankai University, Tianjin 300071, China*

*<sup>d</sup>SCUT-HKUST Joint Research Institute, State Key Laboratory of Luminescent Materials and Devices, South China University of Technology, Guangzhou 510640, China*

*<sup>e</sup>AIE Institute, Guangzhou Development District, Huangpu, Guangzhou 510530, China.*

**‡** These authors equally contributed to this work.

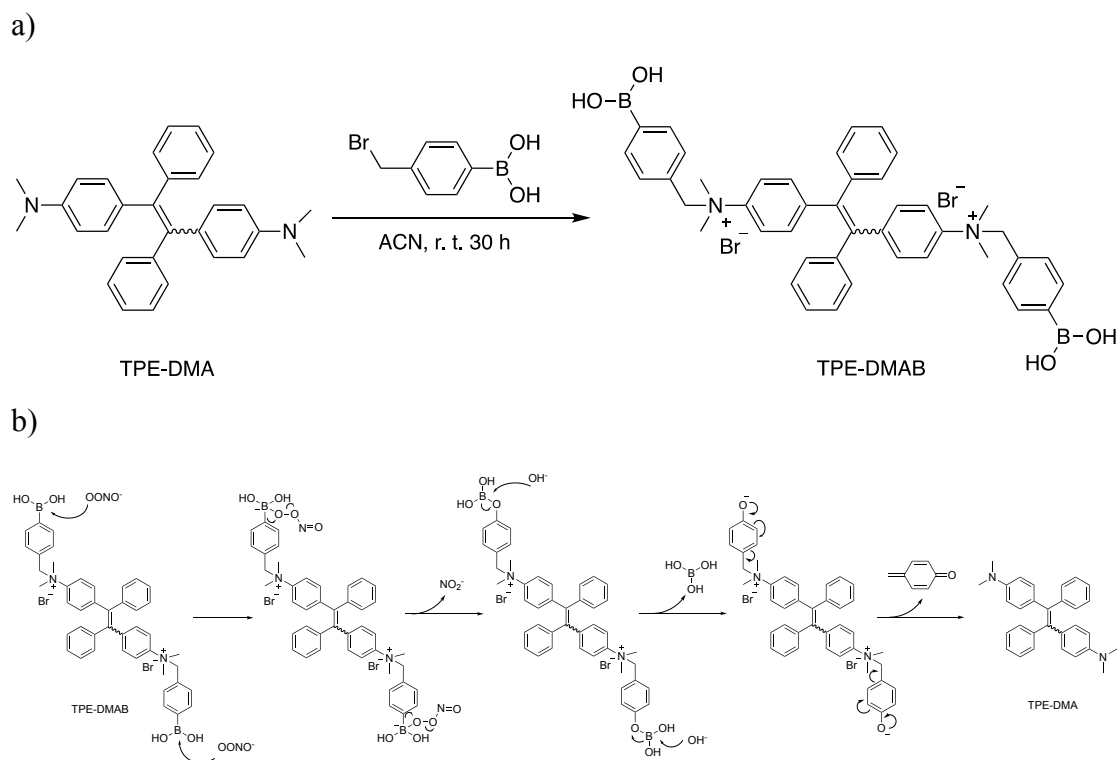


**Fig. S1** a) Synthetic route to TPE-DMAB. b) Proposed mechanism of conversion from TPE-DMAB to TPE-DMA in the presence of  $\text{ONOO}^-$ .

### Generation of various RONS:

The different RONS were generated according to the literature<sup>S1</sup>.

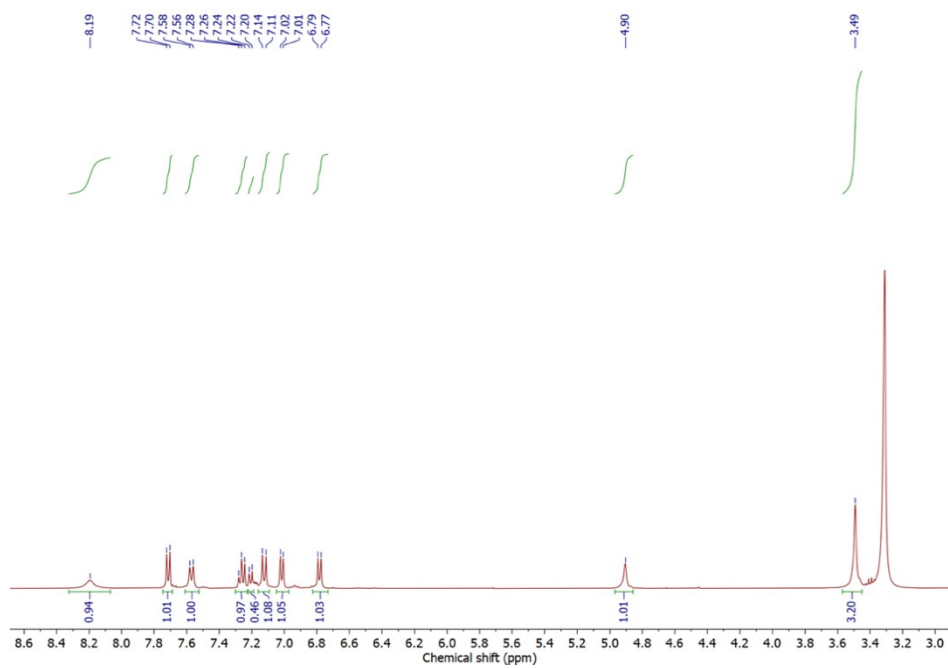


**Fig. S2**  $^1\text{H}$  NMR spectrum ( $\text{CD}_3\text{OD}$ , 400 MHz, 298 K) of TPE-DMAB.

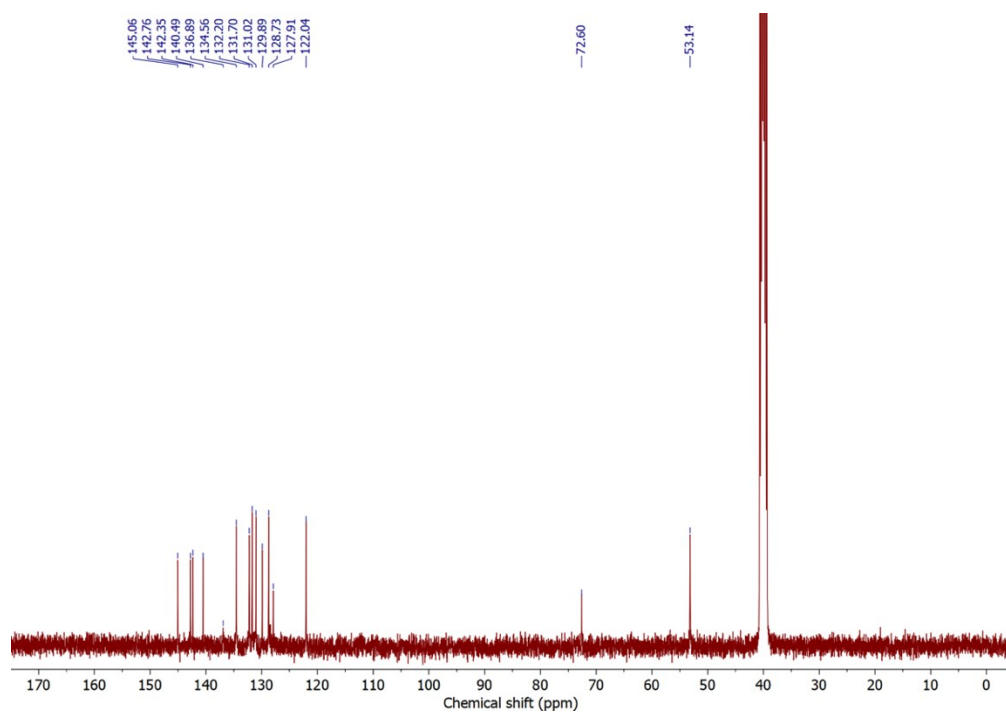


**Fig. S3**  $^{13}\text{C}$  NMR spectrum ( $\text{CD}_3\text{OD}$ , 400 MHz, 298 K) of TPE-DMAB.

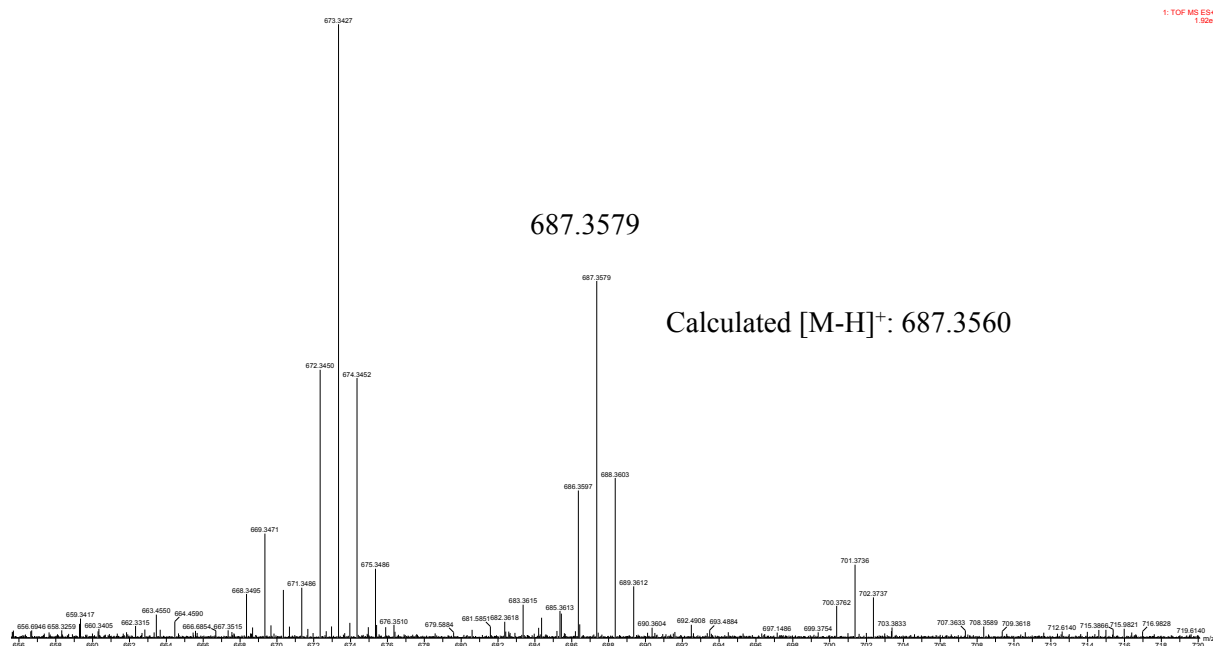


**Fig. S4** ESI mass spectrum of TPE-DMAB.

### Determination of detection limit<sup>S2</sup>

The detection limit was calculated based on the fluorescence titration curve of TPE-DMAB in the presence of ONOO<sup>-</sup> (0-20  $\mu$ M). The fluorescence intensity of TPE-DMAB was measured eleven times and the standard deviation of the measurement was achieved. The detection limit was calculated by the following equation:

$$\text{Detection limit} = 3\sigma/\text{slope} = 54 \text{ nM}$$

Where  $\sigma$  is the standard deviation of the blank measurement, slope is the slope between the fluorescence ratios versus ONOO<sup>-</sup> concentrations.

### Preparation of TPE-DMAB NPs<sup>S3</sup>

1,2-distearoyl-sn-glycero-3-phosphoethanolamine-N-[methoxy(poly-ethylene glycol)-2000] (DSPE-PEG<sub>2000</sub>) as the encapsulation matrix. When a DMSO solution of TPE-DMAB and DSPE-PEG<sub>2000</sub> was added to water under continuous sonication, AIE nanoparticles would form through self-assembly. After dialysis, the AIE nanoparticles

were further purified by ultrafiltration and by passing samples through a 0.3  $\mu\text{m}$  syringe filter to afford the TPE-DMAB NPs.

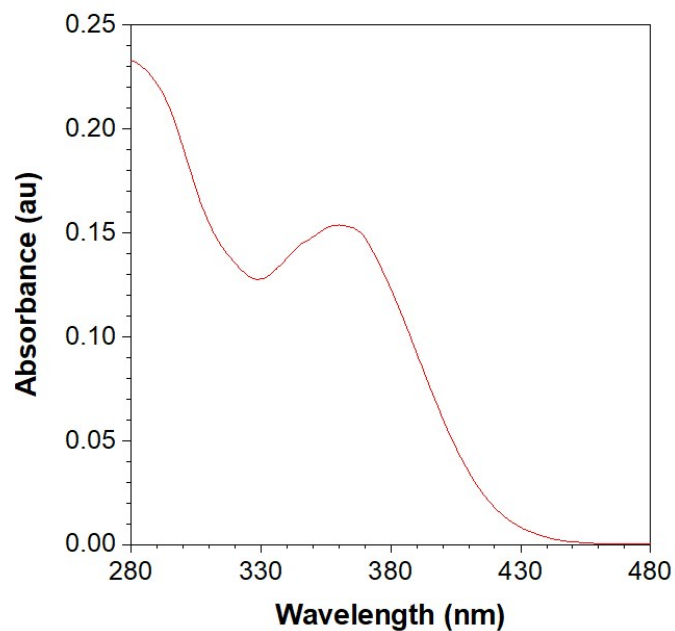


**Fig. S5** Absorption spectrum of TPE-DMA (10  $\mu\text{M}$ ) in THF.

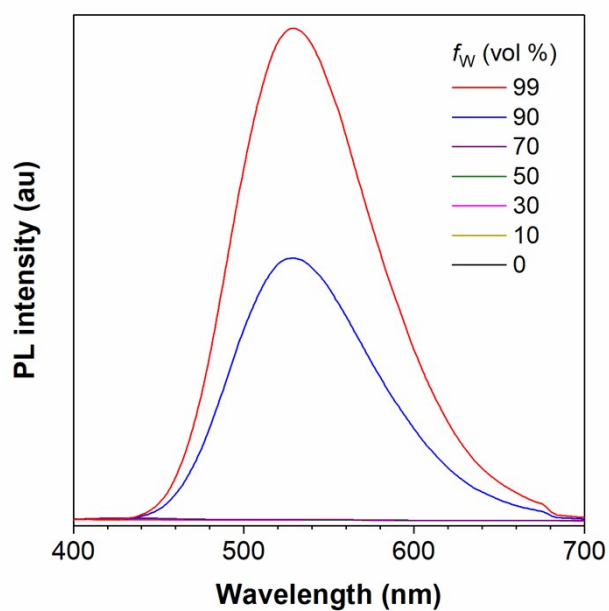


**Fig. S6** PL spectra of TPE-DMA (10  $\mu\text{M}$ ) in THF/water mixtures with different water fractions ( $f_w$ ). Excitation wavelength: 360 nm.

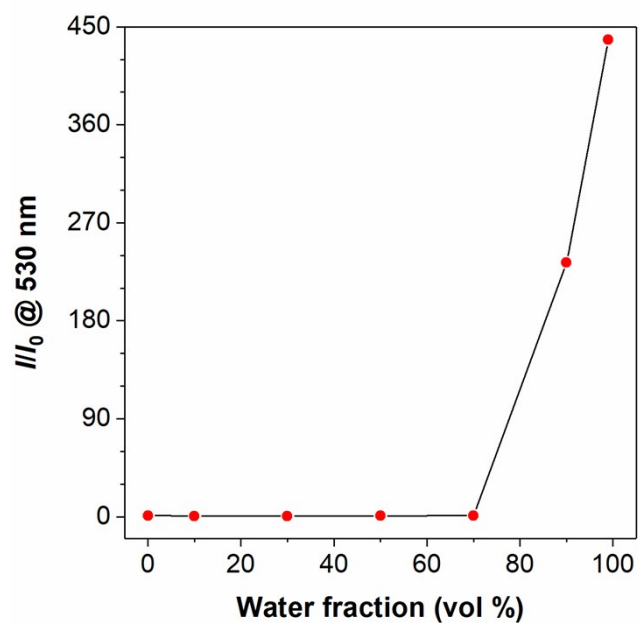


**Fig. S7** Plot of  $I/I_0$  in THF/water mixtures versus water fractions.  $I_0$  and  $I$  are the PL intensities of TPE-DMA ( $10 \mu\text{M}$ ) in THF and THF/water mixtures, respectively.

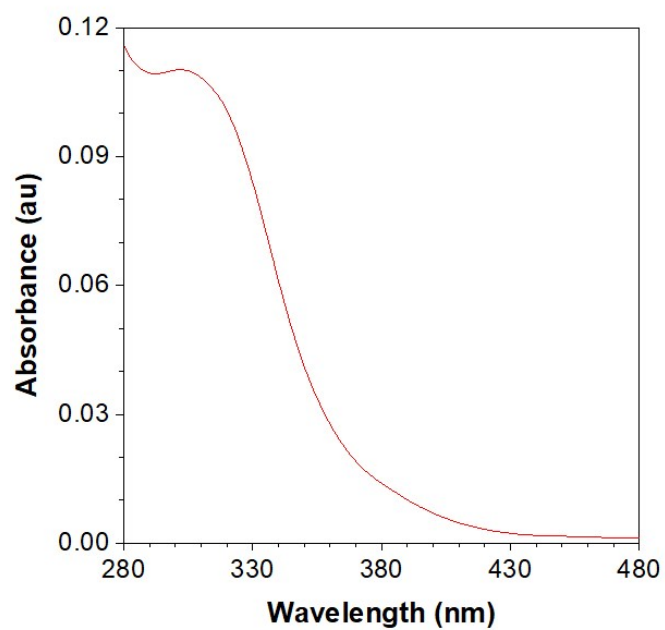


**Fig. S8** Absorption spectrum of TPE-DMAB ( $10 \mu\text{M}$ ) in DMSO.

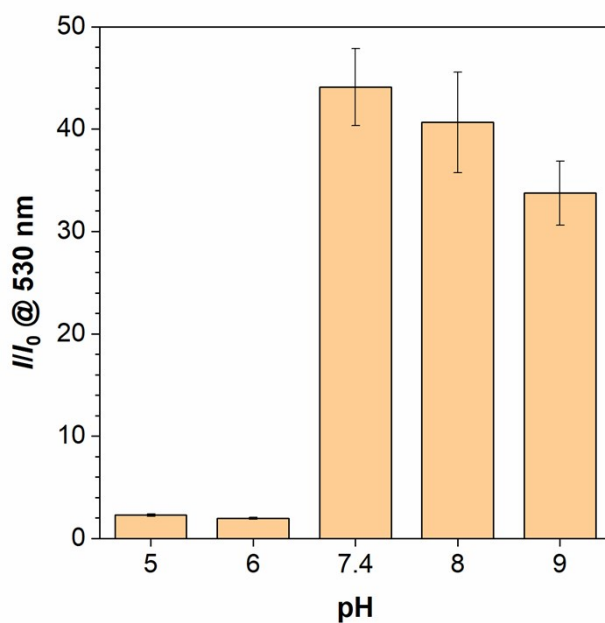


**Fig. S9** Effect of pH of TPE-DMAB (10  $\mu$ M) on  $I/I_0$  in the presence of  $\text{ONOO}^-$  (10  $\mu$ M).  $I$  and  $I_0$  are the PL intensities with and without addition of  $\text{ONOO}^-$ , respectively. Incubation time: 10 min.

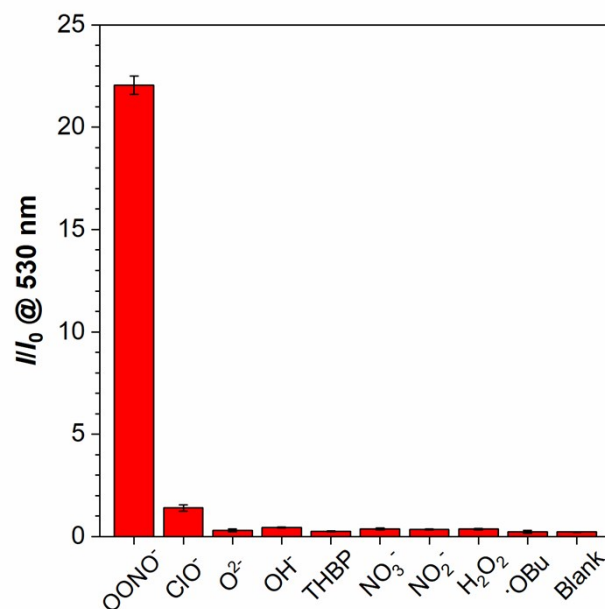


**Fig. S10** Plot of  $I/I_0$  versus various reactive oxygen and nitrogen species (RONS) in PBS buffer (pH 7.4).  $I$  and  $I_0$  are the PL intensities of TPE-DMAB NPs in the presence and absence of RONS, respectively. Incubation time: 10 min.

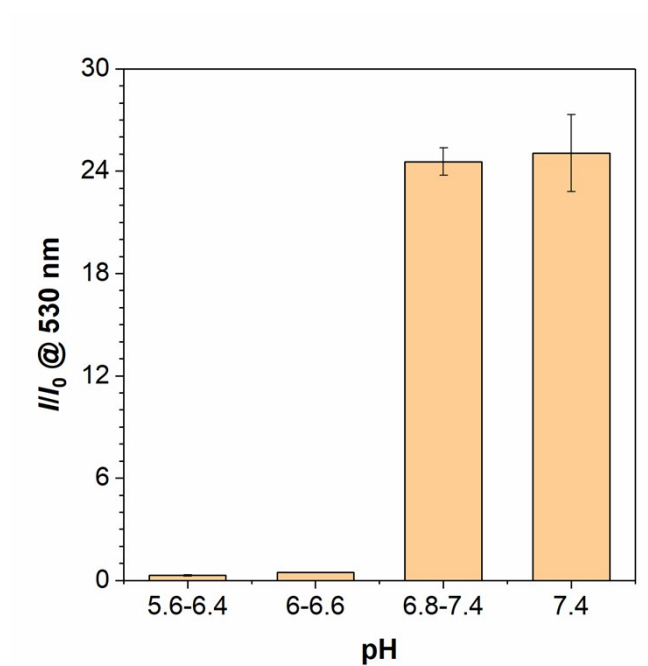


**Fig. S11** Effect of pH of TPE-DMAB NPs on  $I/I_0$  in the presence of  $\text{ONOO}^-$ .  $I$  and  $I_0$  are the PL intensities with and without addition of  $\text{ONOO}^-$ , respectively. Incubation time: 10 min.

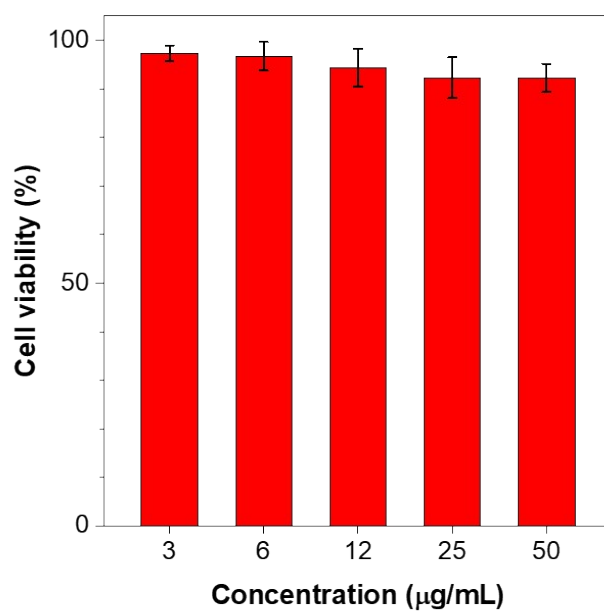


**Fig. S12** Cytotoxicity experiments: TPE-DMAB NPs were evaluated on 4T1 cell by MTT assay. Incubation time: 6 h.



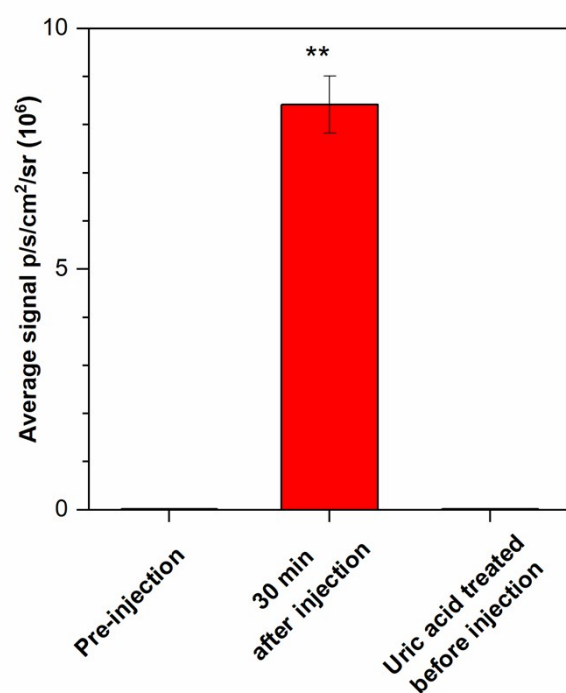


**Fig. S13** The quantified average fluorescence in the infected skins from mice injected with TPE-DMAB NPs (n = 3). \*\* represents  $P < 0.01$  versus TPE-DMAB NPs injected. LPS (1 $\mu$ g) in PBS buffer was injected 4h before administration of TPE-DMAB NPs.

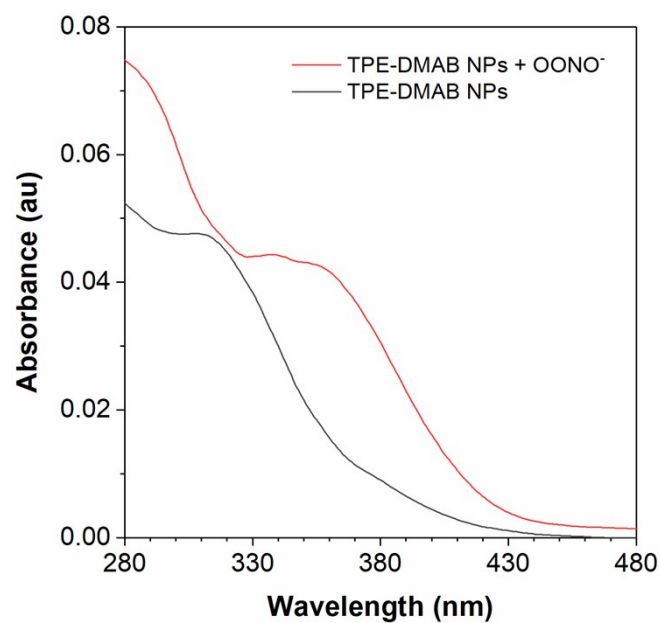


**Fig. S14** Absorption spectra of TPE-DMAB NPs with and without ONOO<sup>-</sup> incubation in PBS buffer (pH = 7.4).

## References

- [S1] X. Jia, Q. Chen, Y. Yang, Y. Tang, R. Wang, Y. Xu, W. Zhu and X. Qian, FRET-based mito-specific fluorescent probe for ratiometric detection and imaging of endogenous peroxynitrite: dyad of Cy3 and Cy5, *J. Am. Chem. Soc.*, 2016, **138**, 10778-10781.
- [S2] W. Zhang, H. Wang, F. Li, Y. Chen, R. T. K. Kwok, Y. Huang, J. Zhang, J. Hou and B. Z. Tang, A ratiometric fluorescent probe based on AIEgen for detecting HClO in living cells, *Chem. Commun.*, 2020, **56**, 14613.
- [S3] D. Ding, C. Goh, G. Feng, Z. Zhao, J. Liu, R. Liu, N. Tomczak, J. Geng, B. Z. Tang, L. G. Ng and B. Liu, Ultrabright organic dots with aggregation-induced emission characteristics for real-time two-photon intravital vasculature imaging, *Adv. Mater.*, 2013, **25**, 6083-6088.